

# The Parametric Current Transformer, a beam current monitor developed for LEP

K. B. Unser, CERN, CH-1211 Geneva 23 (Switzerland)

**Abstract:** Toroidal transformers are used to measure the beam current in beam lines and accelerators. Placing such a transformer in the feedback loop of an operational amplifier will increase the useful frequency range (active current transformer). A magnetic modulator can be added to extend the response to DC current, maintaining with a control loop the transformer core at a zero flux state. The magnetic modulator in the parametric current transformer gives not only the DC response but provides parametric signal amplification up to a transition frequency of about 500 Hz. The low frequency channel (magnetic modulator) and the high frequency channel (active current transformer) are linked together in a common feedback loop. A large dynamic range together with good linearity and low distortion is obtained. This arrangement protects the magnetic modulator from dynamic errors in case of a sudden beam loss, which could impair its zero stability. Dynamic overload protection is an important condition to obtain high resolution and good zero stability, even in applications which require in principle only a very limited frequency response.

## Introduction

Beam current transformers are among the oldest examples of beam instrumentation. Their development has followed the evolution of particle accelerators. Two important milestones of this development should be mentioned here:

The current transformer was placed in the feedback loop of an operational amplifier (H. Hereward and J. Sharp<sup>1</sup>). This extended the low frequency range by a factor approximately equal to the gain of this amplifier. The differentiation time constant  $L/R$  of the "Active Current Transformer" could exceed 1000 seconds, making it possible to measure the circulating beam in the proton synchrotron during several seconds with a negligible shift of the baseline.

A magnetic modulator<sup>2</sup> and a control loop was added to prevent any magnetic flux change in the core of the active beam current transformer. This "zero flux DC current transformer" was originally developed for beam current measurements in the ISR<sup>1</sup>, a storage ring, where the proton beams would circulate for days and weeks. It is an example of a technology developed for particle accelerators which has found many industrial applications<sup>3</sup> for precision DC and AC current measurements.

A new generation of beam current monitors<sup>5</sup> was developed for the LEP project. This gave the opportunity to introduce a number of new ideas to improve the performance and to reduce the influence of environmental factors like stray magnetic fields, electromagnetic interference and mechanical vibrations (microphony). The new instrument is called the Parametric Current Transformer (PCT), because the magnetic modulator provides parametric amplification in the low frequency channel, up to a transition frequency of about 500 Hz.

The development work was done in collaboration<sup>7</sup> with an industrial company in France (technology transfer) who intended to produce this instrument commercially. This meant that a number of economical factors had to be considered which were of lower importance in earlier projects. The priorities for a commercial product are cost, reliability and performance - in that order! The new design goal was to reconcile these requirements without sacrificing the performance. This was achieved by reducing the number of components and their cost (cables,

connectors, electronic components and circuit boards) and by cutting down on the volume, the weight and the power consumption.

This paper gives a summary of the new techniques which are now available for DC beam current measurements. It does not necessarily imply that all of them are required in every practical application.

### System description

The simplified block diagram (Fig. 1) of the PCT system shows 3 distinct transformers and their associated circuits:

- the zero flux transformer ( $T_5$ ) together with the L/R integrator circuit.
- the magnetic modulator ( $T_1, T_2, T_3$ ) with excitation generator and demodulator.
- the ripple feedback transformer ( $T_4$ ) for the ripple compensation circuits.

The transformers are surrounded by electrostatic screens and some of the windings are screened from each other to eliminate unwanted coupling. Current feedback and calibration windings are common to all transformers. Inductive coupling with the beam is symbolically indicated with a one turn beam coupling winding.

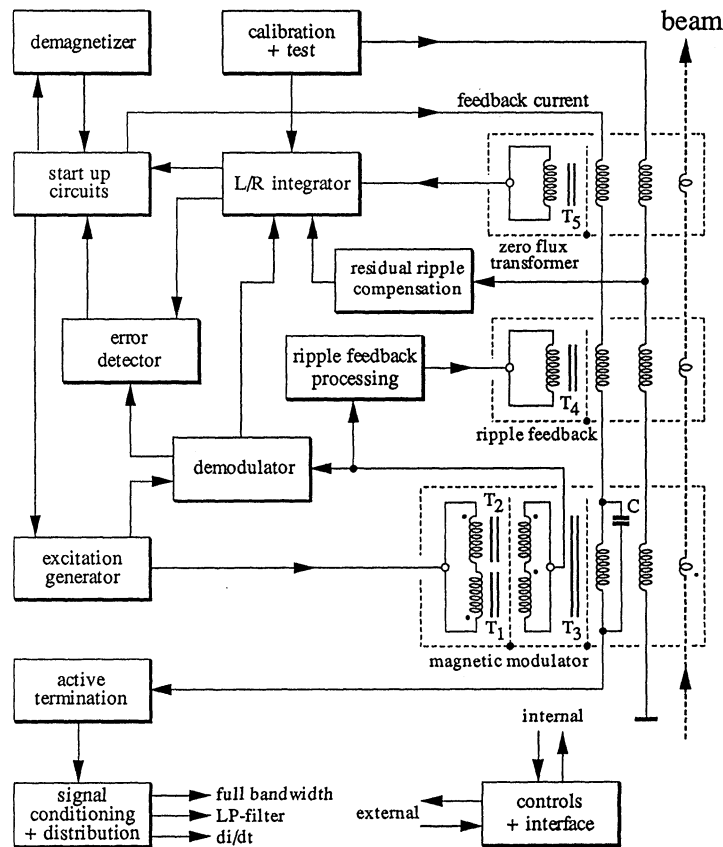


Fig. 1. Simplified block diagram of the PCT

## 268 The Parametric Current Transformer

The magnetic cores are demagnetized (depolarized) automatically each time the mains power is applied. The demagnetizer generates a sinusoidal 50 Hz current ( $>12 A_{pp}$ ) in the feedback windings and this current decays exponentially with a time constant of a few seconds. Demagnetization of the modulator cores is enhanced by programming the excitation generator simultaneously to the highest amplitude before bringing it progressively down to the normal excitation level.

Demagnetizing is important for the zero flux transformer to define the working point close to the center of the B/H loop. This helps to reduce microphony effects, where mechanical vibrations produce a modulation of the residual (remanent) flux and generate parasitic signals. The microphony effects, without this precaution, are very disturbing and could limit the resolution of the monitor in a practical application (vicinity of vacuum pumps etc.).

The magnetic modulator has a memory of previous exposure to a large current. This is probably due to a residual remanence effect. Zero readings may change by more than 1 mA after measuring a current of 1 A, which was, for some reason, not compensated by feedback. This is not only a static offset error, but it is followed by a tendency to drift back during days in the direction of the original zero state. Demagnetization at low frequency permits erasure of this memory effect with an residual error of less than  $\pm 2 \mu A$ .

The zero remanence state of the magnetic cores has to be maintained under all operating conditions. This is the task of the start-up circuits, which apply the feedback current after the demagnetizing cycle is completed, on condition that there is no error signal from the circuits in the feedback loop. Error signals are generated if an excessive external current is applied. This is also transmitted as an error message to the control interface. The error detector has the additional function to supervise the positive and the negative power supplies. A drop in power causes an immediate controlled shut-down followed by a demagnetizing cycle when the power is restored again.

The calibration circuit applies a precision current source to the calibration windings. This is useful as a system test and permits the calibration of the entire data acquisition chain (for both polarities) in a typical application. There is also another function of this circuit: in the control state "test", a known current is added to the current in the feedback windings. The feedback current will try to compensate the error caused by this current source. The change in the zero reading of the PCT can be used to calculate the internal d.c. loop gain of the PCT.

Fast current changes (beam or feedback current) are shorted out with capacitor C, which is decoupled<sup>4</sup> from the modulator with the help of an additional transformer core T3. This capacitor both protects the magnetic modulator from fast transients and attenuates at the same time high frequency components in the modulator output signal, which are coupled into the feedback current loop. This coupling, an undesirable effect, is the origin of modulator ripple in the PCT output signal. A processed modulator output signal is returned back via the ripple feedback transformer to compensate this unwanted signal at the source (reduction up to 98%).

Earlier instruments<sup>4</sup> of this type required a complete 19"- crate with 8 plug-in modules to house the electronics. The new design, in spite of many additional circuit functions, requires only 2 Eurocards (100 × 160 mm) with 4 micro modules in surface mount technology. The total power consumption was reduced by 94% and is now only 3 watts (at zero input current). The electronics is placed in a sealed box without ventilation holes (185 × 130 × 70 mm).

The interconnection between the front-end electronic box and the back-end chassis is a single cable with 3 shielded wire pairs. The first carries the analog signals, the second the power supply and the third the multiplexed bidirectional controls and the power for the demagnetizer. The back-end chassis contains only the analog signal conditioning and distribution circuits, the control interface and the power supply.

### The Magnetic Beam Sensor

The magnetic beam sensor consists of 5 separate magnetic cores, packed together in the toroid assembly (Fig. 2). The cores are strip wound toroids having a useful cross-section between 5 and 25 mm<sup>2</sup> depending on the application. Small cross-sections of the cores were possible thanks to the choice of a high modulation and transition frequency of the system. The soft magnetic material is a thin ribbon (5 mm wide, 23 μm thick) of Vitrovac<sup>®</sup> 6025\*, an amorphous magnetic alloy with the composition (CoFe)<sub>70</sub>(MoSiB)<sub>30</sub>. This material features higher values of permeability and can be used at higher frequencies than conventional (crystalline) nickel/iron alloys.

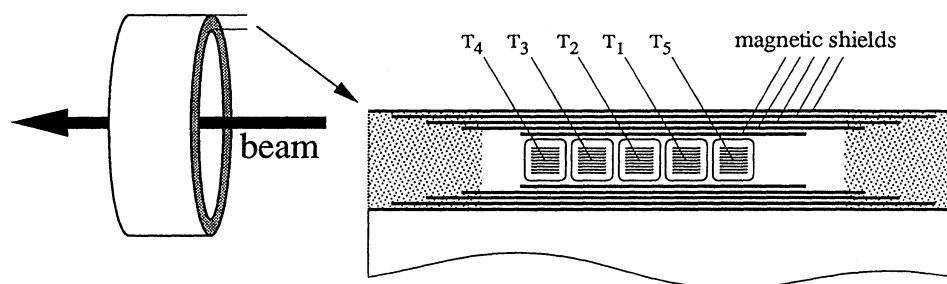


Fig. 2. Toroid assembly, simplified cross-sectional view (windings not shown)

The cores for the 2nd-harmonic magnetic modulator ( $T_1$  and  $T_2$ ) are the most critical components of the system and the magnetic properties of these cores determine the resolution and the zero stability of the instrument. Vitrovac<sup>®</sup> 6025 is now produced in quantity, but the normal commercial grade has a very large spread of magnetic characteristics. A special quality is selected by the manufacturer using a detailed set of specifications containing among others the following selection criteria:

- low value of magnetostriction ( $\lambda_s < 0.2 \times 10^{-6}$ )
- low value of saturation flux density ( $B_s < 0.5$  Tesla)
- good surface quality
- no brittleness

The selected material is submitted to a series of tests to determine the specific annealing conditions<sup>5</sup> for each production batch and the important parameters for the modulator application, i. e. the modulator gain and the magnetic modulator noise. The magnetic noise (Barkhausen noise) depends essentially on the number and the structure of the magnetic domains in the material, which can change with the composition and the annealing treatment of the material. Less than 5% of the material received will pass these tests, but the rest can be used for all other applications, where these specific characteristics are not relevant.

Certain aspects of the fabrication of the cores have been treated in an earlier publication<sup>5</sup> and will not be repeated here. The winding of the modulator cores is a very critical operation. The ribbon has to be continuously controlled with the microscope for mechanical defects (micro fractures and surface defects). The correct winding tension has to be carefully maintained. The insulation between the layers, a mylar foil of 2 μm thickness, is very delicate and difficult to handle. It has to be placed with great care to maintain a minimum and equal spacing between

\* Vitrovac<sup>®</sup> 6025 is a trade name of Vacuumschmelze GMBH, D-6450 Hanau, Germany

## 270 The Parametric Current Transformer

the layers. It is not only necessary to wind all cores with exactly the same number of layers, but also to position the start and the finish of the ribbon in a well defined position in respect of each other. The magnetic ribbon is not simply cut at  $90^\circ$  to the longitudinal axis of the tape but at a very narrow angle in order to distribute the discontinuity in the cross-section over a larger circumference. The finished cores are vacuum impregnated and cross field annealed. The toroidal excitation winding is applied and all magnetic parameters are measured and recorded. Core pairs are selected by matching the dynamic hysteresis loop to better than 1% (defined by the factor of attenuation of the modulation frequency in the common output winding).

The magnetic modulator, in the center of the assembly, is a very sensitive magnetometer to external magnetic fields. This is an undesirable feature which can only be attenuated by extensive magnetic shielding. The magnetic shield of the PCT consists of a number of concentric magnetic cylinders of different length, inside and outside the magnetic cores (Fig. 2). The shields which are closest to the cores consist of several layers of Vitrovac 6025 and provide the best shielding factor, but this material is only available with a maximum width of 50 mm. All other shields are Mumetal. Seen in this context, the small cross section of the magnetic cores is also an important advantage for efficient magnetic shielding. It helps to bring the inner and the outer shields closer together and reduces the volume of the magnetic beam sensor.

This shielding attenuates the external field by a factor between 50 to 500, depending on the number of shields in use. This is not enough in many applications. One has also to consider that high permeability shields are easily saturated by a strong external magnetic field.

### The Excitation Generator

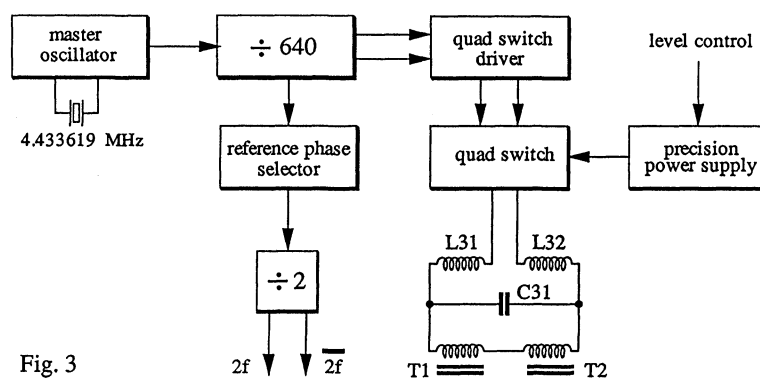


Fig. 3

**Basic design consideration:** The resolution and zero drift of the PCT should only be limited by the magnetic noise of the magnetic modulator. The contribution of noise from the electronic circuits should ideally be considerably lower. As a design limit, the tolerance for these contributions have been arbitrarily set to  $\leq 10$  nA rms of equivalent beam current.

This translates into the following specifications for the excitation generator (assuming matching errors  $\leq 1\%$  for the modulator core pair):

- variation of 2nd harmonic distortion:  $\leq 5$  ppm
- variation of frequency:  $\leq 10$  ppm
- variation of amplitude:  $\leq 50$  ppm (parts per million)

The excitation frequency of the magnetic modulator should be as high as possible, but eddy currents in the core material impose an upper limit which is in our case around 7 kHz.

A crystal controlled master oscillator (Fig 3) with a stability  $\leq 3$  ppm and a synchronous divider generate the excitation frequency ( $f = 6927.3$  Hz). The tolerance is less than 1 ns for the differential timing error (difference in duration of the positive and the negative half period) and less than  $100 \mu\text{V}$  for the differential amplitude error. The difference of rise and fall times and the corresponding transmission delays of the digital control signals have to be taken into account. A perfect symmetry of all pulse forming elements is required and symmetric transmission lines for the timing signals are used. The circuit board lay-out is critical. A quad DMOS transistor array (on a single chip) in a symmetrical H-bridge configuration<sup>5</sup> is used to switch the output of a precision regulated power supply. A passive low pass filter (L31; L32 and C31) eliminates the higher frequency components. The capacitor C31 supplies high current peaks (Fig. 4) in an avalanche discharge to drive the cores hard into saturation and recuperates a large part of the stored energy on the return swing. The optimum value of this capacitor and the optimum value of peak excitation current as a function of resolution are individually determined for each magnetic sensor in a semi-automatic test set up.

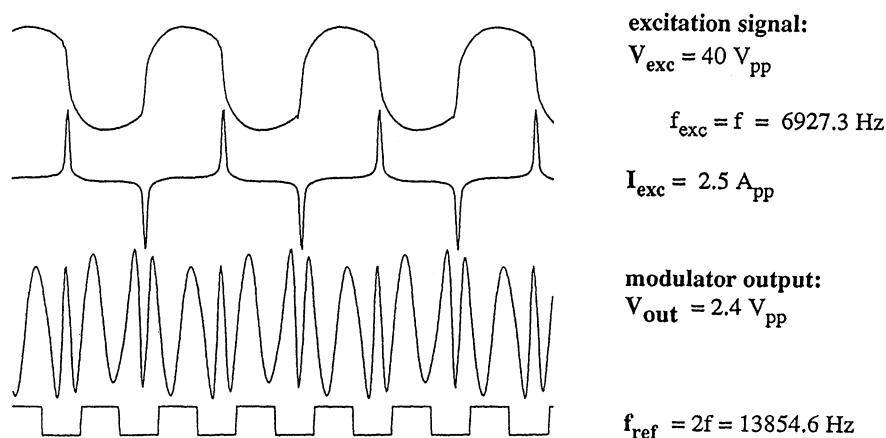


Fig. 4. Typical signal waveforms observed on a magnetic modulator (plot of display, averaged signals, on LeCroy 9410 oscilloscope). The core matching in this example is better than 0.5%. The exact waveform of the output signal is an individual "signature" for every magnetic modulator.

### The Demodulator

The demodulator has to detect and to amplify the 2nd harmonic component in the output signal of the modulator. It has to satisfy the following specifications, taking into account the parametric amplification<sup>5</sup> in the magnetic modulator:

Resolution:       $0.1 \mu\text{V rms}$  (for a bandwidth of 1 Hz)  
                       $10 \mu\text{V rms}$  (for a bandwidth of 500 Hz)

This 2nd-harmonic signal is completely masked by a parasitic output (see Fig. 4) of the magnetic modulator, resulting from the core matching error of the magnetic modulator. This parasitic signal is composed of the modulation frequency  $f$  and a spectrum of odd harmonics (3f; 5f; 7f; 9f; 11f etc.). It has an amplitude of several volts, more than 150 dB higher than the required resolution for the 2nd harmonic signal.

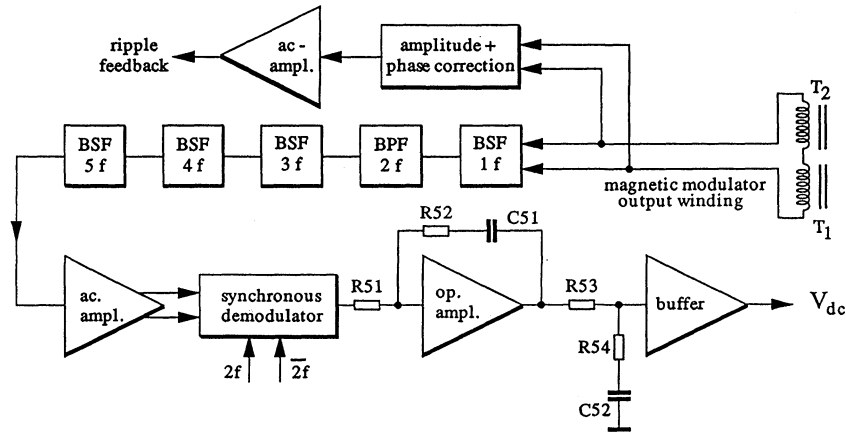


Fig. 5. Simplified block diagram of demodulator

To obtain the specified resolution, it is necessary to attenuate, with a filter, the parasitic signals by more than 50 dB and to amplify the 2nd harmonic component at least 30 dB before demodulation. The bandwidth of the filter should be 2.5 kHz above and below  $2f$  in order to accommodate the upper and lower sidebands of the modulated signal with an acceptable phase error. This is one of the conditions which has to be satisfied to make the overall feed-back loop stable, considering a transition frequency of 500 Hz for the low frequency channel.

The filter is a passive LC-network and consist of 1 band pass (BPF) and 4 band stop (BSF) sections. The signal, after demodulation in a synchronous detector, is integrated with the time constant  $R51 \times C51$  for a 6 dB/octave (frequency) roll-off. This determines the transition (cross-over) frequency between the modulator channel and the active current transformer channel.

### The Active Current Transformer

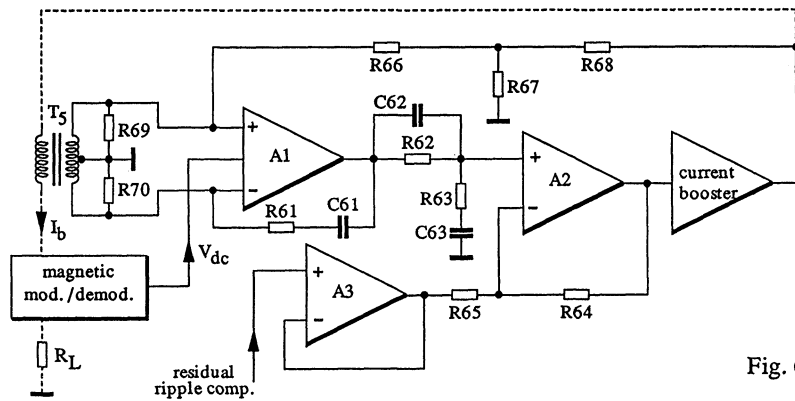


Fig. 6

The active current transformer with the zero flux transformer ( $T_5$ ) and the overall feedback loop of the PCT is shown in Fig. 6. The signal gain for medium and high frequencies (up to 1 MHz) is provided by a composite amplifier (the L/R integrator), consisting of A1; A2 and a current booster for max. 100 mA. The DC and low frequency gain comes from the magnetic modulator/demodulator in cascade with a part of the high frequency channel. The 2 channels have therefore 2 independent inputs, but one common output and one common feedback loop, which defines the (closed loop) signal gain of the system. The signal path is always via the channel with the highest open loop gain at any particular input frequency.

Considerations of loop stability impose an upper frequency limit ( $< 1/10 f$ ) for the transition from the low to the high frequency channel. A high transition frequency has many advantages. It reduces the required core cross-section for the zero flux transformer  $T_5$ , limits the noise contribution of amplifier (A1) and reduces the microphony effect of core  $T_5$ . All these effects increase rapidly at lower frequencies.

The open loop gain of both cascaded channels is very high ( $> 150$  dB at DC). This is how good linearity, low distortion and the large dynamic range of the PCT is obtained. It requires a carefully tailored roll off (gain and phase) in the direction of the unity gain cross over frequency (1 MHz) of the system. Phase correction elements in the active current transformer (R61, C61 - R62, C62 - R63, C63) and in the demodulator (R52, C51 - R53, R54, C52) have to be set for optimum loop stability and a clean step response. Range switching does not influence the dynamics of the feedback loop, because the (virtual) load impedance  $R_L$  is constant and small.

Damping resistors (R69 and R70) eliminate undesirable high frequency resonances of the zero flux transformer  $T_5$ . They cause a small gain error (2 to 3 %) in this channel, which is compensated by a corresponding amount of positive feedback (via R66, R67 and R68).

The parasitic output signal of the magnetic modulator, coupled into feedback loop, causes an unwanted error current (modulator ripple) in this loop. This effect is unfortunately enhanced by the low output impedance of the current buffer and the low value of (virtual) load impedance ( $R_L = 50$  ohms). The ripple feedback via  $T_4$ , mentioned earlier, reduces this effect already by a large factor. The remaining ripple signal is measured at the calibration winding and added via A3 and A2 to the signal of the current booster (compensation by "bootstrapping").

### The Active Termination

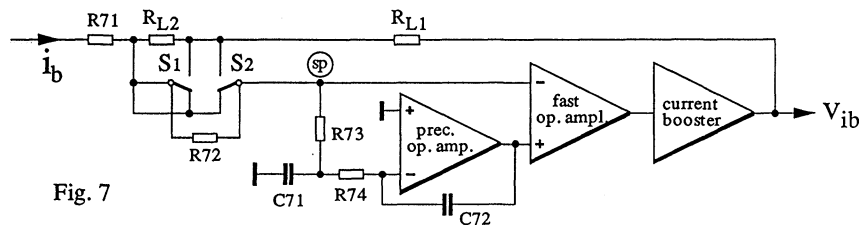


Fig. 7

The active termination converts the feedback current  $i_b$  into an output voltage  $V_{ib}$ . Two precision load resistors ( $R_{L1}$  and  $R_{L2}$ ) in the feedback loop of an operational amplifier provide a virtual ground reference at the summing point (sp). The operational amplifier is in reality a composite amplifier with a separate high and low frequency channel and a current booster (100 mA max.). This arrangement permits an accurate measurement of the average beam current, even if the input signal consists of very short pulses, separated by a long time interval.

The switches S1 and S2 select the current ranges A and B without interrupting the

feedback path and without adding the contact resistance to the load resistor values. The load resistors  $R_{L1}$  and  $R_{L2}$  are composed of several precision resistors in parallel in order to keep the power dissipation in each of them at a low level. Resistor  $R_{71}$  ( $50 \Omega$ ) defines the actual impedance of this active termination in the main feedback loop and keeps it at a constant and low value to reduce the effects of parasitic capacitance of the different elements in this loop, a condition for loop stability, independent of the selected current range

### Signal conditioning and distribution

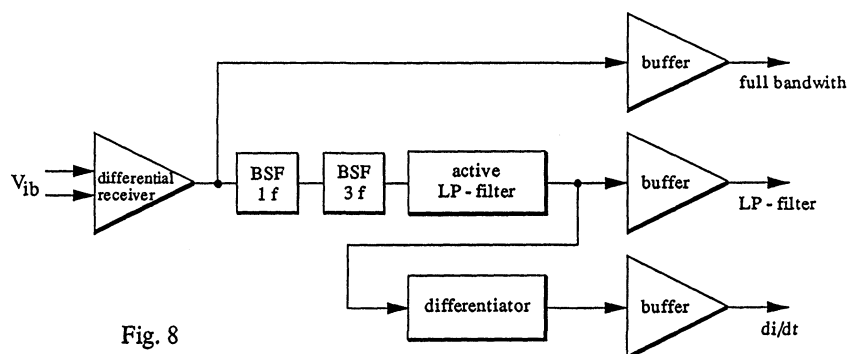


Fig. 8

The analog signal  $V_{ib}$  from the front end is transmitted over a symmetrical transmission line, up to a distance of several hundred meters. A differential line receiver rejects all common mode noise which may be present on the line. The signal path is either direct or via a low pass filter and optional band stop filters<sup>6</sup> (BSF) for  $f$  and  $3f$  to reject spurious modulator noise. A differentiated signal, proportional to beam loss, is also provided. There is a buffer amplifier for every signal output.

### Results

The following specifications can be obtained with a selected sensor:

Sensor dimension	225 mm o.d. 175 mm i.d. 100 mm length
Range A, full scale	any range from 10 mA to 100 A (both polarities)
Range (B)	1 to 20 % of range A
Linearity error *	$\pm 0.001 \%$ $\pm$ zero error
Resolution *	$\pm 0.3$ ppm of range (A) $\pm 0.4 \mu\text{A rms}$ ( $\pm 1 \mu\text{A rms}$ typical)
Zero drift *	$\pm 1 \mu\text{A}/^\circ\text{C}$ ( $\pm 5 \mu\text{A}/^\circ\text{C}$ typical)
Zero drift (24 h) *	$\pm 2 \mu\text{A rms}$ (at constant temperature)
Bandwidth	DC to 100 kHz
Accuracy (calibration source)	$\pm 0.05 \%$

\*) measurements with a 1 sec. integration window

Resolution and zero drift are not at all limited by the electronics, but depend only on the quality of the magnetic sensor. The quality of the Vitrovac 6025 material is in this respect of crucial importance. Material purchased 5 years ago gave in general better results than that currently produced at present. One observes very different zero drift behavior among sensors which are built with exactly the same batch of material. This is an indication, that all the factors

which influence these characteristics are not as yet clearly identified.

The temperature drift is not so much caused by the temperature coefficient of the material itself than by the uneven mechanical constraints in the two modulator cores. The temperature dependent zero drift is generally reduced after a period of artificial ageing (temperature cycling between 20°C and 80°C) and the temperature coefficient of the sensor becomes in any case more reproducible. It is a good idea to incorporate a temperature gauge in the beam sensor, if the temperature drift is critical in a particular application.

During long term zero drift test one can sometimes observe in intervals of several hours or days a fairly sudden change of up to 2  $\mu$ A. The cause of these phenomena are not known.

### Acknowledgments

Many people have made their contributions: C. Bovet and R. Jung gave their support to the project and many useful discussions are gratefully acknowledged. The computer controlled test bench for dynamic testing of core samples was designed and built by P. Buksh. The mechanical design of the core winding machine and the different tooling required in the project was first the responsibility of A. Maurer and at a later date of G. Burtin.

J. Bergoz, A. Charvet, R. Lubès and P. Pruvost (BERGOZ, F-01170 Crozet, France) designed circuit lay-outs and built the different prototypes. They made experiments with the different construction methods for the magnetic cores and the toroid assembly and performed an incredibly large number of tests to find the optimum annealing procedures. Their practical experience in building a large number of PCT's is a valuable help for any future improvements.

G. Herzer, R. Hilzinger, W. Kunz and R. Wengerter (Vacuumschmelze GMBH, D-6450 Hanau, Germany) contributed with their knowledge of amorphous magnetic alloys and helped with the selection of a suitable quality of Vitrovac material.

### References

1. K.B. Unser, "Beam current transformer with DC to 200 MHz range", **IEEE Trans. Nucl. Sci.**, NS-16, June 1969, pp. 934-938.
2. F.C. Williams, S.W. Nobel, "The fundamental limitations of the second-harmonic type of magnetic modulator as applied to the amplification of small DC signals", **Journal. IEE (London)**, vol. 97, 1950, pp. 445-459.
3. H.C. Appelo, M. Groenenboom, J. Lisser, "The zero flux DC current transformer, a high precision wide-band device", **IEEE Trans. Nucl. Sci.**, Vol. N.S.-24, No.3, June 1977, pp. 1810-1811.
4. K.B. Unser, "A toroidal DC beam current transformer with high resolution", **IEEE Trans. Nucl. Sci.**, NS-28, No. 3, June 1981, pp. 2344-2346.
5. K.B. Unser, "Design and preliminary tests of a beam intensity monitor for LEP" **Proc. IEEE Particle Accelerator Conference**, March 1989, Chicago, Vol. 1, pp. 71-73.
6. R.L. Witkover, "New beam instrumentation in the AGS booster", April 22-24, 1991, KEK, Tsukuba, Japan: **Proceedings of the Workshop on Advanced Beam Instrumentation**, Vol. 1, pp. 50-59.
7. Collaboration contract K 017/LEP (CERN/BERGOZ) Geneva, December 1986.